

ARTICLES

Competition between Pauli and orbital effects in a charge-density-wave system

J. S. Qualls,¹ L. Balicas,^{2,3} J. S. Brooks,² N. Harrison,⁴ L. K. Montgomery,⁵ and M. Tokumoto⁶

¹*Department of Physics, Wake Forest University, Winston-Salem, North Carolina 27109*

²*National High Magnetic Field Laboratory, Florida State University, Tallahassee, Florida 32306*

³*Universidad Simón Bolívar, Departamento de Física, Caracas 1080A, Venezuela*

⁴*National High Magnetic Field Laboratory, LANL, MS-E536, Los Alamos, New Mexico 87545*

⁵*Department of Chemistry, Indiana University, Bloomington, Indiana 47405*

⁶*Electrotechnical Laboratory, Tsukuba, Ibaraki 305, Japan*

(Received 8 October 1999)

We present angular-dependent magnetotransport and magnetization measurements on α -(ET)₂MHg(SCN)₄ compounds at high magnetic fields and low temperatures. We find that the low-temperature ground state undergoes two subsequent field-induced density-wave-type phase transitions above a critical angle of the magnetic field with respect to the crystallographic axes. This new phase diagram may be qualitatively described assuming a charge-density-wave ground state which undergoes field-induced transitions due to the interplay of Pauli and orbital effects.

Low-dimensional electronic systems characterized by a quasi-one-dimensional (Q1D) Fermi surface tend to form either a charge-density-wave (CDW) or a spin-density-wave (SDW) ground state at low temperatures as a consequence of one-dimensional instabilities.^{1,2} High magnetic fields have proven to be useful to investigate, and even manipulate, these ground states, since the effects are quite different for the CDW and the SDW cases. The Zeeman (Pauli) energy is expected to suppress a CDW state because a CDW couples only bands with the same spin. In a magnetic field it is not possible to have the same nesting wave vector \mathbf{Q} for both spin-up and spin-down bands (see Ref. 3). In analogy with the Pauli effect in superconductors,⁴ the Zeeman energy, $\mu_B^2 \rho(E_F) B^2$ [where $\rho(E_F)$ is the density of states at the Fermi level], competes with the CDW condensation energy, $-\rho(E_F) \Delta(0)^2$. The transition temperature is expected to decrease with increasing field, and above a certain threshold field [$\approx \Delta(0)/\mu_B$] a uniform CDW is no longer energetically favorable. Consequently, a CDW may be suppressed by high magnetic fields. In contrast, for a SDW system, the nesting property is not affected by the Zeeman term because a SDW couples spin-up with spin-down states. The nesting condition is actually improved by high magnetic fields due to the magnetic-field-induced one-dimensionalization of the Q1D electronic orbits. Thus for an imperfectly nested Fermi surface, the SDW transition temperature can actually increase with increasing magnetic field.^{5,6} The role of orbital effects on SDW systems has been well established in the Q1D organic Bechgaard salts.⁷

By using a simple BCS relation, we can obtain a rough estimate for the critical field necessary to suppress a uniform CDW: $B_c = 1.765 k_B / \mu_B T_c$, where k_B is the Boltzmann constant, μ_B is the Bohr magneton, and T_c is the transition temperature to the DW state. However, the relatively high transition temperatures (≥ 30 K) of most CDW systems, such as,

for example, the molybdenum bronzes,² implies the need for very high magnetic fields, of the order of 100 tesla or more, in order to suppress the CDW ground state via the Zeeman energy. This limitation has prevented the observation of this field-induced suppression. In this work, we argue that the α -(ET)₂MHg(SCN)₄ (where $M = \text{K, Tl, and Rb}$) organic conductors may be the *first* compounds whose ground state is driven towards new DW states under the influence of *both* Pauli and orbital effects in available fields.

The band-structure calculations⁸ of α -(ET)₂MHg(SCN)₄ indicate the presence of both closed Q2D and open Q1D orbits at the Fermi energy E_F . It is generally accepted that these systems undergo a phase transition from a metallic phase to a low-temperature DW state⁹⁻¹¹ at a transition temperature, T_{DW} , between 8 and 12 K. The onset of this second-order transition at T_{DW} (Ref. 12) is known to decrease with increasing field, as would be expected for a CDW transition.¹³ Also, below T_{DW} and at intermediate magnetic fields (between 22 and 37 tesla), there are profound changes in the magnetoresistance which are indicative of a first-order phase transition in the electronic structure at the so-called “kink transition field,” B_K . This critical field clearly indicates that a magnetic field has a profound effect on the ground state of these compounds. Above B_K , T_{DW} remains finite (~ 2 K) (Refs. 13–15) up to fields as high as 45 tesla.¹⁶ After nearly a decade, the identity of the low-temperature ground state remains a contemporary issue, with conflicting evidence supporting both CDW and SDW scenarios.¹⁷ There is published experimental data which, at first glance, seem to support a SDW-like ground state: The muon spin relaxation (μSR) rate¹¹ changes below T_{DW} while the magnetic susceptibility is found to be anisotropic below the same temperature.¹⁰ Nevertheless, no line broadening or line splitting is observed either on the nuclear magnetic resonance¹⁵ or on the electron-spin-resonance¹⁸ spec-

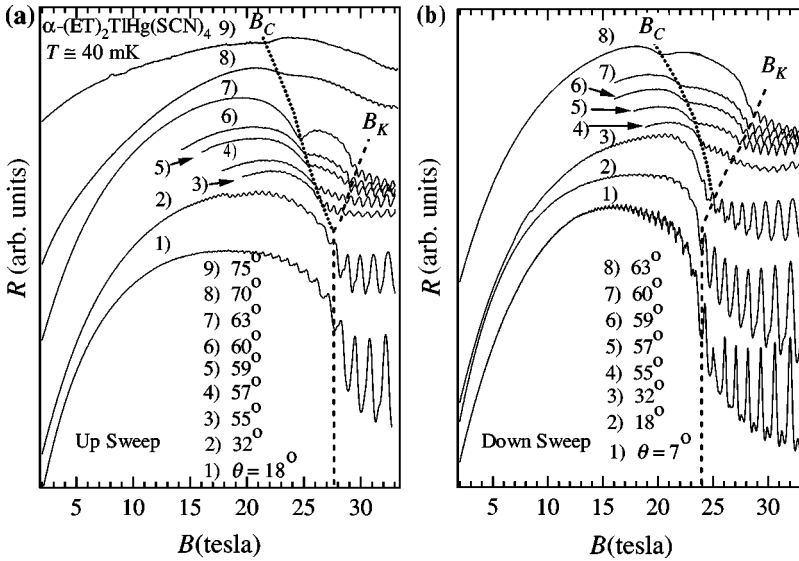


FIG. 1. (a) Magnetoresistance, $R(B)$, of an α -(ET) $_2\text{TIHg}(\text{SCN})_4$ single crystal as a function of magnetic field B , at $T=40$ mK, for increasing field sweeps at several angles θ between B and \mathbf{b}^* (θ is indicated in the figure). (b) Same as in (a) but for decreasing field sweeps. Dashed line indicates B_K while the dotted line indicates B_c . In both figures curves are vertically displaced for clarity.

trum below T_{DW} . The existence of 2D closed orbits, clearly seen in de Haas–van Alphen measurements,¹⁹ can generate Landau diamagnetism, which could be responsible for the anisotropy in the magnetic susceptibility. Thus the anisotropy alone cannot be taken as definitive proof for a SDW ground state. On the other hand, no x-ray or neutron-diffraction data that could support the existence of either a CDW or SDW superstructure have thus far been published. Clearly, there is a lack of compelling experimental evidence providing unambiguous support for either of the two DW ground-state scenarios.

In this paper we study the angular dependence of the magnetoresistance and magnetization of the α -(ET) $_2\text{MHg}(\text{SCN})_4$ system. Our study reveals features, in particular a magnetic-field-induced electronic phase transition, which appear only when the angle θ , defined as the angle between the magnetic field and the \mathbf{b}^* axis, satisfies the condition $\theta = \theta_c \geq 45^\circ$. Furthermore, the kink field, B_K , displays a nontrivial angular dependence for $\theta \geq \theta_c$. We therefore propose a B - θ phase diagram and argue that it appears to be well explained by present theoretical models describing the behavior of a CDW under high magnetic fields with competing Pauli and orbital effects.^{20,21}

Single crystals of α -(ET) $_2\text{MHg}(\text{SCN})_4$ (M is K, Tl, or Rb) were grown using conventional electrocrystallization techniques.⁷ Transport measurements were made using four-terminal methods with currents ranging from $1 \mu\text{A}$ up to $10 \mu\text{A}$ applied perpendicular to the conducting layers (along the \mathbf{b}^* axis). Meanwhile, the magnetization measurements were performed using a phosphor-bronze cantilever magnetometer. Various configurations of cryostats, magnets, and rotating inserts available at the National High Magnetic Field Laboratory in both Tallahassee and Los Alamos were used in this investigation.

The magnetoresistance, $R(B)$, for α -(ET) $_2\text{TIHg}(\text{SCN})_4$ as a function of tilted magnetic field, B , at $T \approx 40$ mK is plotted in Fig. 1. Figures 1(a) and 1(b) show the up- and down-field sweeps, respectively. At small angles, the familiar behavior of the magnetoresistance as a function of field strength is observed. This includes a rapid rise in resistance which reaches a maximum around 15 tesla, followed by a drop in resistance which terminates at B_K , near 27 tesla (up-sweep) or 24 tesla (down-sweep). B_K (indicated in the figure by a dashed line) is hysteretic, and is characteristic of a magnetic-field-induced first-order change in electronic structure. It is easily identifiable because the amplitude and

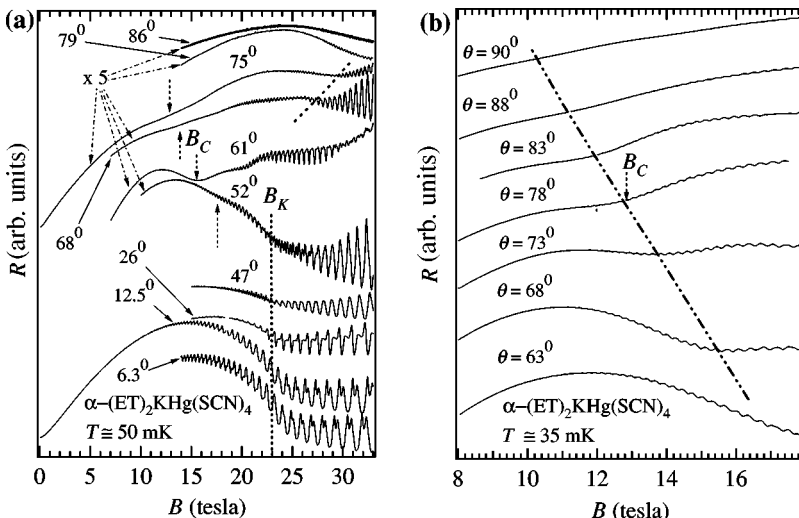


FIG. 2. (a) $R(B)$ for an α -(ET) $_2\text{KHg}(\text{SCN})_4$ single crystal as a function of B at $T=50$ mK for increasing field sweeps and several values of θ (indicated in the figure). B_K is indicated by a dashed line while dotted arrows indicate B_c . (b) $R(B)$ as a function of B , on an amplified scale, for a second α -(ET) $_2\text{KHg}(\text{SCN})_4$ single crystal at $T=35$ mK and for different values of θ as indicated. The line indicates B_c . In both figures, curves are vertically displaced for clarity while in (a) all curves for $\theta \geq 52^\circ$ are multiplied by a factor of 5.

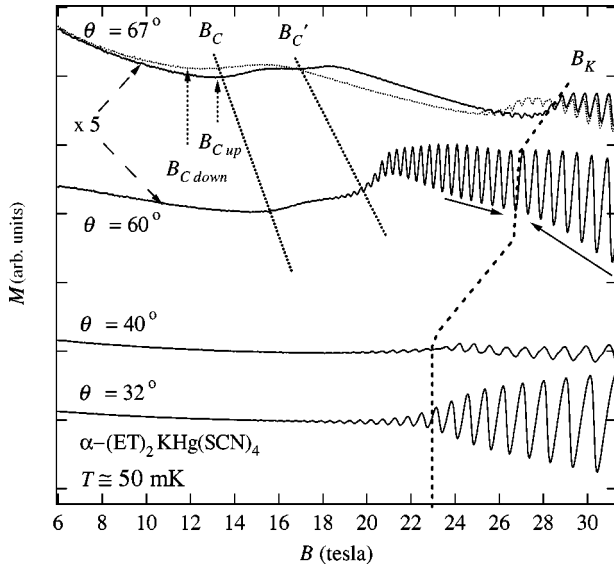


FIG. 3. Magnetization, M , of an $\alpha\text{-(ET)}_2\text{KHg(SCN)}_4$ single crystal as a function of B at $T=500$ mK and for four values of θ . All curves are displaced vertically while the curves at $\theta=60^\circ$ and 67° are multiplied by a factor of 5. B_K is indicated by a dashed line while B_c is indicated by both dotted line and dotted vertical arrows. Solid arrows indicate the place of B_K for $\theta=60^\circ$. All solid lines are for increasing field sweeps. The dotted line at $\theta=67^\circ$ indicates a decreasing field sweep. B'_c , also indicated by a dashed line, suggests an additional phase transition.

wave form of the Shubnikov–de Haas (SdH) oscillations change abruptly at this point. For large angles, B_K shifts to higher fields and an additional hysteretic structure (hereafter termed B_c and indicated in the figure by a dotted line) begins to appear. Notably, B_c shifts to lower fields with increasing angle. We argue below that both B_K and B_c are connected with first-order transitions between sub-phases of the density wave ground state. In retrospect, evidence of B_c has been observed before, but was mislabeled as B_K .²²

To further establish the universal character of these sub-phases, we provide similar results for the $\alpha\text{-(ET)}_2\text{KHg(SCN)}_4$ compound. Figure 2(a) plots $R(B)$ as a function of B (for increasing field sweeps) at $T\approx 50$ mK for several values of θ (θ is indicated in the figure) for a single crystal of $\alpha\text{-(ET)}_2\text{KHg(SCN)}_4$. The values of B_c and B_K are indicated by dotted arrows and a dashed line, respectively. Both fields display a strong angle dependence, which is qualitatively similar to that discussed in Fig. 1. Notice that at $\theta=86^\circ$, B_K is outside the accessible field range. The behavior of B_c and B_K is reproducible and observed in multiple samples. In Fig. 2(b), the behavior of B_c is shown on an amplified scale for yet another crystal, at $T=35$ mK and for values of θ between 63° and 90° . For the $\alpha\text{-(ET)}_2\text{KHg(SCN)}_4$ compound and for θ close to 60° , the field position of B_K is ambiguous. This will be the subject of future efforts.

The thermodynamic nature of B_K and B_c , as transitions between subphases, was verified by magnetization measurements made on a third sample of $\alpha\text{-(ET)}_2\text{KHg(SCN)}_4$. Figure 3 shows the magnetization, M , as a function of B at $T=0.5$ K for several values of θ . As previously seen in Figs. 1 and 2(a), B_K (indicated by a dashed line) moves towards

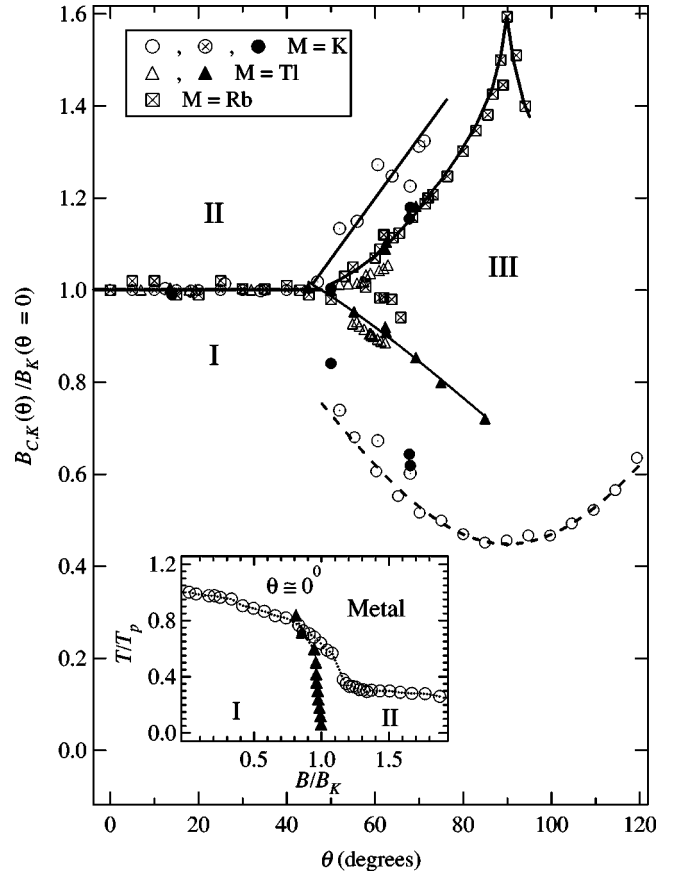


FIG. 4. (a) $B_c(\theta)$ as well as $B_K(\theta)$, both normalized with respect to $B_K(\theta=0)$, for each sample shown in Figs. 1 and 2. Solid and opened triangles are $B_c(\theta)$ and $B_K(\theta)$, respectively, obtained from Fig. 1. Similarly, solid and opened circles were obtained from Fig. 2 and other $\alpha\text{-(ET)}_2\text{KHg(SCN)}_4$ samples, while squares correspond to B_K measured in an $\alpha\text{-(ET)}_2\text{RbHg(SCN)}_4$ sample at $T=3.0$ K. The resulting B - θ phase diagram is composed of three regions. Solid lines are guides to the eyes and suggest first-order phase transitions. The dashed line (also indicating first order) is a fit to the expression for B_{cy} , see the text. Inset: T_{DW} from Ref. 9 normalized with respect to T_{DW} at zero field, as a function of B/B_K for $M=K$ (circles). We added new points for $B/B_K \geq 1.1$ as well as the position of B_K in this phase diagram (solid triangles).

higher fields as θ increases above $\sim 40^\circ$. For fields between 12 and 20 tesla, we observe further structure that is indicated by vertical dotted arrows and agrees with values of B_c observed in Fig. 2. For $\theta=67^\circ$, both field-up (solid line) and field-down (dotted line) sweeps are included to show the hysteretic behavior of both B_K and B_c . Although no pronounced discontinuities are observed in $M(B)$, the hysteretic behavior points towards a *first-order* phase transition at both critical fields. Furthermore, the magnetization reveals additional fine structure at B'_c and may indicate the existence of another subphase. As in Fig. 2(a), B_K cannot be easily determined for θ near 60° .

In Fig. 4, the angular dependence of both $B_c(\theta)$ and $B_K(\theta)$ is plotted for $\alpha\text{-(ET)}_2\text{TIHg(SCN)}_4$ (triangles) and for $\alpha\text{-(ET)}_2\text{KHg(SCN)}_4$ (circles). The figure also includes $B_K(\theta)$ obtained for an $\alpha\text{-(ET)}_2\text{RbHg(SCN)}_4$ single crystal (squares) at $T=3.0$ K for fields up to 50 tesla.²³ To enable a comparison between all three salts, we have normalized

$B_c(\theta)$ as well as $B_K(\theta)$ with respect to the compound-dependent $B_K(\theta=0)$. The result is a B - θ phase diagram containing three distinct regions. The hysteretic phase transition at $B_K(\theta)$, indicated by a solid line, is identified as a *first-order* phase transition from the zero-field ground state (region I) to a distinct high-field phase (region II). For angles larger than $\sim 45^\circ$, a new phase (region III) emerges between regions I and II. The hysteresis in Figs. 1 and 3 associated with B_c indicates that the transition between regions II and III is also *first order*. The field dependence of B_K is very different from that of B_c . B_K is cusplike near $\theta=90^\circ$.

Recently, the magnetic-field dependence of a Q1D system with a CDW ground state was studied theoretically^{20,21} using a mean-field approach. In this theory, both CDW and SDW correlations were included in an anisotropic 2D Hamiltonian and studied in the random-phase approximation. An important parameter of the theory is $\eta \equiv q_0/q_p = e b v_F \cos \theta / \mu_B$, defined as the ratio between the orbital and Pauli contributions to the nesting vector \mathbf{Q} . The predictions of this model strongly resemble the experimentally determined phase diagram of α -(ET)₂MHg(SCN)₄, where $M = \text{K, Tl, or Rb}$. In particular, the theory predicts (using the author's notation) that (i) below a second-order transition temperature, T_{c0} , the ground state is a uniform charge density wave CDW₀; (ii) above a critical field, there is a first-order transition^{20,21} at B_{cx} to a high-field state CDW_x, which is a *hybrid of charge- and spin-density-wave* states; (iii) between CDW₀ and CDW_x, a new phase CDW_y is stabilized that is dependent on θ through $B_{cy} \approx B_c^0 \sqrt{1 + 0.088 \eta^2}$; and (iv) all subphase transitions are first order (CDW_y is expected *not* to have SDW character). We find a close match of the above theory to the experimental phase diagram of α -(ET)₂MHg(SCN)₄, if we assign T_{DW} to T_{c0} and B_K to B_{cx} , implying that region I corresponds to the CDW₀ state and region II to the high-field CDW_x phase. In effect, according to Ref. 20, the Pauli effect should suppress the critical temperature, T_{DW} , from the metallic phase towards region I (CDW₀ state) in proportion to the square of the magnetic field.^{3,13,20,21} This is evident in the T - B phase diagram of the α -(ET)₂KHg(SCN)₄ compound as shown in the inset of Fig. 4. Here, T_{DW} (normalized with respect to its zero-field value) is plotted as a function of B/B_K for $M = \text{K}$ at $\theta = 0^\circ$ taken from Ref. 9. In the same

plot, additional data points are included from the onset of an abrupt change in slope of $R(B)$ as a function of T for $B/B_K \geq 1.1$.¹⁶ Solid triangles indicate the position of B_K in this diagram. As has been previously pointed out,^{3,20,21} the theoretical T - B phase diagram is remarkably similar to the diagram shown in the inset of Fig. 4. To further strengthen the correlation between theory and experiment, we note that the above expression for B_{cy} may be fitted to the data for B_c from $M = \text{K}$ (see the dashed line in Fig. 4) with the parameters $B_c^0 \approx 10.4$ tesla and a Fermi velocity $v_F = 1.8 \times 10^5$ m/s. This is close to the value from band-structure calculations⁸ and implies well (but *not* perfectly) nested Q1D Fermi sheets for the α -(ET)₂MHg(SCN)₄ salts (where $M = \text{K, Tl, or Rb}$).

In summary, we have closely examined the angular-dependent magnetoresistance and magnetization in the low-temperature DW ground state of α -(ET)₂MHg(SCN)₄ (where $M = \text{K, Tl, or Rb}$). We find that the material exhibits at least three low-temperature electronic subphases, which are separated by first-order phase boundaries. We argue that for low fields and tilted angles, the ground state is well represented by a CDW description (albeit that no direct evidence for a CDW as opposed to a SDW presently exists). For $\theta \geq \theta_c \approx 45^\circ$, we identify a new structure, B_c , seen in the angular dependence of both magnetoresistance and magnetization, as a field-induced phase transition governed by the competition between orbital and Pauli effects. The appearance of this new phase at θ_c displaces B_K (given by the Pauli limit) towards higher values. The B - T and B - θ phase diagrams are well described by the available models for charge-density waves in high magnetic fields. This study both supports theoretical predictions of the complex behavior of CDW in a magnetic field and clarifies the nature of the ground state in the α -(ET)₂MHg(SCN)₄ compounds.

The authors thank N. Biřkup for helpful discussions, and recognize the cooperation received from S. Y. Han, Brian H. Ward, Yuri Sushko, and the staff of NHMFL-LANL. In addition, we acknowledge support from NSF-DMR 95-10427 and 99-71474 (J.S.B.). One of us (L.B.) is grateful to the NHMFL for sabbatical leave support. The NHMFL is supported through a cooperative agreement between the State of Florida and the NSF through NSF-DMR-95-27035.

¹V. J. Emery, in *Highly Conducting One Dimensional Solids*, edited by J. T. Devreese, R. P. Evrard, and V. E. Van Doren (Plenum, New York, 1979), p. 247; J. Solyom, *Adv. Phys.* **28**, 201 (1979); *Electronic Properties of Inorganic Quasi-One-Dimensional Compounds*, edited by P. Monceau (Reidel, Dordrecht, 1985).

²C. Schlenker, in *Low Dimensional Electronic Properties of Molybdenum Bronzes and Oxides* (Kluwer, New York, 1989).

³R.H. McKenzie, cond-mat/9706235 (unpublished).

⁴B.S. Chandrasekhar, *Appl. Phys. Lett.* **1**, 7 (1962); A.M. Clogston, *Phys. Rev. Lett.* **9**, 266 (1962).

⁵L.P. Gor'kov and A.G. Lebed, *J. Phys. (France) Lett.* **45**, L433 (1984).

⁶A. Audouard and S. Askenazy, *Phys. Rev. B* **52**, R700 (1995); A. Bjelis and K. Maki, *ibid.* **44**, 6799 (1991).

⁷T. Ishiguro, J. Yamaji, and G. Saito, in *Organic Superconductors* (Springer-Verlag, Berlin, 1998); J. Wosnitza, *Fermi Surfaces of Low-Dimensional Organic Metals and Superconductors* (Springer-Verlag, Berlin, 1996).

⁸H. Mori *et al.*, *Bull. Chem. Soc. Jpn.* **63**, 2183 (1990); L. Ducasse and A. Frisch, *Solid State Commun.* **91**, 201 (1994); R. Rousseau *et al.* *J. Phys. I* **6**, 1527 (1996).

⁹T. Sasaki *et al.*, *Solid State Commun.* **75**, 93 (1990); T. Sasaki, S. Endo, and N. Toyota, *Phys. Rev. B* **48**, 1928 (1993); P.F. Henning *et al.*, *Solid State Commun.* **95**, 691 (1995); M. Köppen *et al.*, *Synth. Met.* **86**, 2057 (1997).

¹⁰T. Sasaki, H. Sato, and N. Toyota, *Synth. Met.* **41-43**, 2211 (1991); P. Christ *et al.*, *ibid.* **86**, 2057 (1997).

¹¹F.L. Pratt *et al.*, *Phys. Rev. Lett.* **74**, 3892 (1995).

¹²P. Henning *et al.*, *Solid State Commun.* **95**, 691 (1995).

- ¹³N. Biškup, J.A.A.J. Perenboom, J.S. Brooks, and J.S. Qualls, *Solid State Commun.* **107**, 503 (1998); M.V. Kartsovnik *et al.*, *Synth. Met.* **86**, 1933 (1997); T. Sasaki, A.G. Lebed, T. Fukase, and N. Toyota, *Phys. Rev. B* **54**, 12 969 (1996).
- ¹⁴M.V. Kartsovnik *et al.*, *Synth. Met.* **86**, 1933 (1997).
- ¹⁵P.L. Kuhns *et al.*, *Solid State Commun.* **109**, 637 (1999); T. Takahashi *et al.*, *Synth. Met.* **55-57**, 2513 (1993); K. Kanoda *et al.*, *ibid.* **70**, 973 (1995); K. Miyagawa, A. Kawamoto, and K. Kanoda, *ibid.* **86**, 1987 (1997).
- ¹⁶J. S. Brooks *et al.* (unpublished).
- ¹⁷J. S. Brooks *et al.*, in *Proceedings of Physical Phenomena at High Magnetic Fields II*, edited by Z. Fizk, L. Gor'kov, D. Meltzer, and R. Schrieffer (World Scientific, Singapore, 1996), p. 249.
- ¹⁸R. Tsuchiya *et al.*, *Synth. Met.* **70**, 965 (1995).
- ¹⁹S. Uji *et al.*, *Solid State Commun.* **12**, 825 (1996).
- ²⁰A. Bjeliš, D. Zanchi, and G. Montambaux, *J. Phys. IV* **9**, 203 (1999); cond-mat/9909303 21 Sep 1999 (unpublished).
- ²¹D. Zanchi, A. Bjeliš, and G. Montambaux, *Phys. Rev. B* **53**, 1240 (1996).
- ²²T. Osada, R. Yagi, A. Kawasumi, and S. Kagoshima, *Synth. Met.* **41-43**, 2171 (1991).
- ²³J. S. Qualls *et al.* (unpublished).